The influence of ocean flow on newly forming sea ice

Daniel L. Feltham

Centre for Polar Observation and Modelling, Department of Space and Climate Physics, University College London,
United Kingdom

M. Grae Worster

Institute of Theoretical Geophysics, Department of Applied Mathematics and Theoretical Physics, University of Cambridge,
United Kingdom

J. S. Wettlaufer[1]

Applied Physics Laboratory and Department of Physics, University of Washington, Seattle, USA

[1]   The heat and mass balance of the Arctic Ocean is very sensitive to the growth and decay of sea ice and the interaction between the heat and salt fields in the oceanic boundary layer. The hydraulic roughness of sea ice controls the detailed nature of turbulent fluxes in the boundary layer and hence is an important ingredient in model parameterizations. We describe a novel mechanism for the generation of corrugations of the sea ice–ocean interface, present a mathematical analysis elucidating the mechanism, and present numerical calculations for geophysically relevant conditions. The mechanism relies on brine flows developing in the sea ice due to Bernoulli suction by flow of ocean past the interface. For oceanic shears at the ice interface of 0.2 s^{-1}, we expect the corrugations to form with a wavelength dependent upon the permeability structure of the sea ice which is described herein. The mechanism should be particularly important during sea ice formation in wind-maintained coastal polynyas and in leads. This paper applies our earlier analyses of the fundamental instability to field conditions and extends it to take account of the anisotropic and heterogeneous permeability of sea ice.   INDEX TERMS: 4207 Oceanography: General: Arctic and Antarctic oceanography; 4540 Oceanography: Physical: Ice mechanics and air/sea/ice exchange processes; 4203 Oceanography: General: Analytical modeling; KEYWORDS: sea ice, sea ice–ocean interface, corrugations, ocean flow, instability

1.   Introduction

[2]   The growth and decay of sea ice in the polar regions is the high-latitude equivalent of the evaporation-precipitation cycle in the remainder of the world's oceans [*Aagaard and Carmack*, 1994]. Sea ice insulates the ocean from the atmosphere, reflects solar radiation, and influences thermohaline circulation. Recent studies of dramatic changes in the ice cover [*McPhee et al.*, 1998; *Morison et al.*, 1998; *Rothrock et al.*, 1999] have refocused attention on the correct parameterization of local processes in numerical modeling studies that have large scale consequences, for example, *Zhang et al.* [1998]. Numerical simulations of sea ice cover typically use one-dimensional models of its thermodynamic evolution that are coupled to models of sea ice motion and deformation in response to wind-induced, oceanic, and internal stress. Thermodynamic models of sea ice vary in complexity, ranging from a simple slab model with linear temperature gradient (the "zero-layer" Semtner model [*Semtner*, 1976]) used in many global circulation studies, to sophisticated models that parameterize the brine content [*Maykut and Untersteiner*, 1971], or treat, for example, melt ponds and lead fraction [*Ebert and Curry*, 1993]. These models were developed in the context of regional or global climate simulations and have led to many important insights. By computational necessity, however, these models have included parameterizations of several physical processes and have omitted others. In this paper, we are interested in investigating the effect of brine flow within the sea ice, which is not treated explicitly in such models. By modeling brine flow, it is possible to predict brine distribution within the sea ice and also to investigate certain flow-induced interactions with the ocean, in particular, the physical basis for turbulent parameterization schemes under rough ice.

[3]   Recent experimental work on brine flows in laboratory-grown sea ice have demonstrated the usefulness of general theories of "mushy layers" [*Wettlaufer et al.*, 1997a, 1997b]. Mushy layers are regions of mixed phase (solid and liquid) in which the solid forms a rigid matrix and the liquid fills and may flow within the interstices. Thus, typically, the whole of a layer of sea ice including the thin, skeletal layer of ice next to the ocean, is a mushy layer. Figure 1 shows a cross-section through laboratory-grown sea ice [*Wettlaufer et al.*, 1997a] which clearly reveals platelets of ice separated by brine inclusions. In addition to sea ice, mushy layers form commonly during the solidification of two-component melts, such as metallic alloys and aqueous salt solutions. Using a mathematical model of a mushy layer, this paper describes the detailed interactions between brine flow in sea ice and the flow of the ocean beneath it. The instability we discuss results in the formation of a corrugated sea ice–ocean interface, and it is predicted to be strongest in young first-year sea ice under conditions of rapid oceanic flow. Therefore we expect that the phenomenon will be particularly important for sea ice which forms in tidally driven fjords or wind-maintained coastal polynyas such as the St. Lawrence Island Polynya. The exposed ocean quickly freezes because of large heat losses to the atmosphere, and as it does so, the forming sea ice layer is blown away from the coast, for

---

[1]Now at Departments of Geology and Geophysics and Physics, Yale University, New Haven, Connecticut, USA.
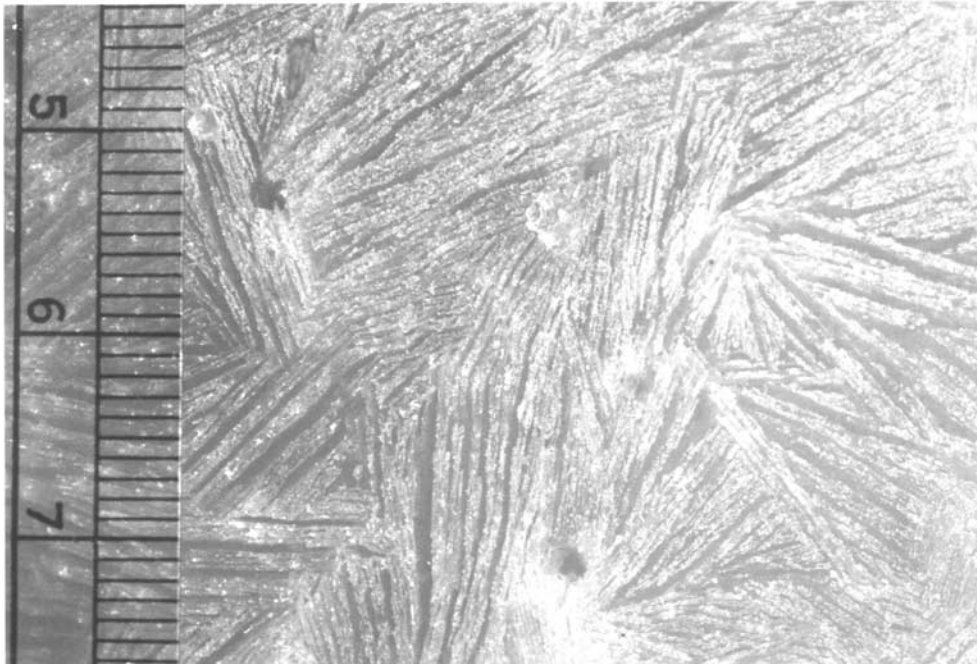
Figure 1. The underside of laboratory-grown sea ice showing ice platelets with c axes that are predominantly horizontal, which restricts horizontal fluid motions relative to vertical ones. The scale on the left is in centimeters. The two circular holes are brine channels. Taken from *Wettlaufer et al.* [1997a].

example, by strong katabatic winds. Numerical calculations of haline convection beneath leads with a forming sea ice cover also give oceanic shears sufficiently large that corrugations are expected to form [*Smith and Morison*, 1993].

2. Flow-Induced Deformation of the Sea Ice−Ocean Interface

[4] We illustrate how ocean flow can cause the sea ice−ocean interface to become corrugated using a simplified mathematical description. Some of the assumptions presented here are relaxed in the analysis of *Feltham and Worster* [1999].

[5] The interstitial brine within sea ice may flow in response to buoyancy forces and pressure gradients. For example, buoyancy-driven convection ("gravity drainage") has been described by *Weeks* [1998] and *Wettlaufer et al.* [1997a, 1997b], and flushing of melt water through the ice during summer is caused by the pressure head of standing melt water on the ice surface [*Untersteiner*, 1968]. Most of the characteristics of brine flow are fundamentally the same as those of flows within porous media [*Phillips*, 1991; *Bear*, 1972], the simplest model of which is given by Darcy's equation

$$\mu \mathbf{u} = \mathbf{\Pi}(-\nabla p + \rho \mathbf{g}). \qquad (1)$$

Here $\mathbf{u}$ is the "Darcy" velocity, which is the volume flux of brine per unit perpendicular, cross-sectional area flowing between the ice crystals, p is the pressure, μ is the dynamic viscosity of the brine, ρ is brine density, and $\mathbf{g}$ is the acceleration due to gravity. The permeability $\mathbf{\Pi} = \mathbf{\Pi}(\phi)$ is a second-rank tensor because the resistance to flow within sea ice is anisotropic and is a function of the brine fraction 1 - ϕ (where ϕ is the solid ice fraction) and the geometry of the internal phase boundaries. We consider the case of anisotropic sea ice such as undeformed congelation ice, the ubiquitous form in the Arctic Ocean, in which the platelets

are aligned perpendicular to the sea ice−ocean interface (the c axes are horizontal). Thus the permeability parallel to the platelets is the permeability to vertical flows Π_v and the permeability to horizontal flows is $\Pi_h = \beta^2 \, \Pi_v$, where $\beta^2 \equiv \Pi_h/\Pi_v \leq 1$ because brine flows more easily parallel to the platelets. The appropriate value of β (where $0 \leq \beta \leq 1$) depends upon the difference in horizontal and vertical permeability along platelets, the difference in horizontal permeability across platelets compared with that along them and the orientation of platelets to the mean ocean flow direction. Since there is typically a steep vertical temperature gradient in newly forming sea ice, there is a gradient in solid fraction and hence permeability, decreasing with temperature toward the sea ice−atmosphere interface. We model this by treating the permeability of the ice layer to be given by a decaying exponential

$$\Pi_v(z) = \Pi_v(0)e^{\gamma z}, \Pi_h(z) = \beta^2 \Pi_v(z), \qquad (2)$$

where the sea ice occupies $z < 0$ ($z = 0$ is the position of the planar sea ice−ocean interface) and γ can be chosen on the basis of observations or treated as a free parameter. Laboratory experiments with newly forming sea ice provide support for this profile and suggest $\gamma G^{-1} \approx 1$ K^{-1}, where G is the temperature gradient in the sea ice [*Ono and Kasai*, 1980]. The brine flow within the sea ice introduces an advection term into the equation expressing local conservation of heat within the sea ice

$$\rho c \frac{\partial T}{\partial t} + \rho c \mathbf{u} \cdot \nabla T = \nabla \cdot (k \nabla T) + \rho \mathcal{L} \frac{\partial \phi}{\partial t}, \qquad (3)$$

where $\mathcal{L}$ is the latent heat released per unit mass as the ice fraction increases, c is the specific heat capacity, k is the conductivity, and ρ is the density of both brine and ice (which, for simplicity, we assume to be equal). Our assumption that the brine and ice densities are equal (and therefore equal to the
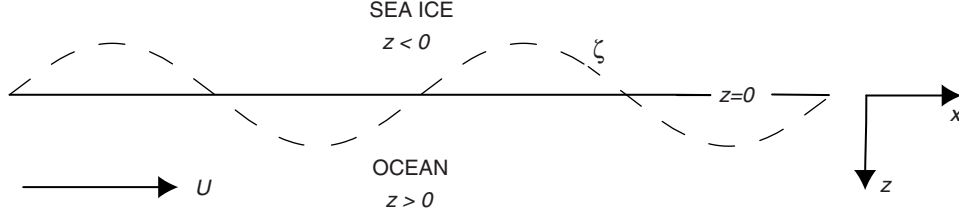
Figure 2. The geometry of the idealized sea ice–ocean system. A semi-infinite layer of sea ice ($z < 0$) floats upon the ocean ($z > 0$), in which there is a uniform flow U parallel to the undisturbed interface. The dashed line shows how the sea ice–ocean interface is perturbed.

ocean density) removes the role of buoyancy forces and allows us to isolate the role that brine flow driven solely by an externally imposed pressure gradient plays in the development of corrugations. Although buoyancy forces will, in general, play an important role in brine drainage, they have been shown to be ineffective during the initial stages of sea ice growth. Only once a critical ice depth has been exceeded does buoyancy drive brine flow and cause the formation of brine channels [*Wettlaufer et al.*, 1997a, 1997b]. This may take as little as 12 hours, during which time ice grown in polynyas could be blown well over a kilometer away from the coast. The evolution of the sea ice–ocean interface is given by the Stefan condition (a heat balance), which is

$$\rho \mathcal{L} \phi v_{\mathbf{n}} = k \mathbf{n} \cdot \nabla \mathrm{T}|_{si} - k \mathbf{n} \cdot \nabla T|_{o}. \tag{4}$$

In this equation, $\mathbf{n}$ is the unit normal at the interface pointing into the ocean, v_n is the normal growth speed of the interface, and the right-hand side is the difference in heat conducted into the interface from the ocean and away from the interface into the sea ice (and eventually to the atmosphere). Note that we have written the heat flux in the ocean as being controlled by conduction, $k \mathbf{n} \cdot \nabla T|_{o}$, which holds in the thin, molecular part of the oceanic boundary layer. This heat flux takes the form of a turbulent flux when the surface and outer parts of the oceanic boundary layer are considered.

[6] The flow in the ocean affects brine flow within sea ice through the pressure it exerts upon the sea ice–ocean interface. To focus attention on the interfacial region, consider a semi-infinite sea ice layer ($z < 0$) floating upon the ocean $z > 0$ which flows with uniform velocity U parallel to the interface. Consider the fate of an incipient corrugation (perturbation) to the sea ice–ocean interface $\zeta = \hat{\zeta} e^{i\alpha x + \sigma t}$, where x is the distance along the undeformed interface, α is the wave number of the perturbation, and σ is its growth rate, see Figure 2. For simplicity, assume that the flow in the ocean is irrotational so that $\mathbf{u} = \nabla \Phi$, where, from continuity, the velocity potential Φ satisfies $\nabla^2 \Phi = 0$. Since the flow of brine in the sea ice is much slower than the flow in the ocean we can treat the sea ice as impermeable to the external flow ($\mathbf{n} \cdot \nabla \Phi = 0$ on $z = \zeta$) and calculate that

$$\Phi = Ux - iU\zeta e^{-\alpha z}. \tag{5}$$

The linearized Bernoulli equation [*Batchelor*, 1967] then gives the pressure at the interface to be

$$p = -\rho\alpha U^2 \zeta. \tag{6}$$

There is lower pressure beneath the crests and higher pressure beneath the troughs of the sea ice–ocean interface, and it is this pressure difference that drives a flow of brine in the sea ice (Figure 3a). By ignoring internal phase change within the sea ice (which follows from the quasi-stationary approximation, $\partial/\partial t \to 0$, see below), continuity of brine flow gives $\nabla \cdot \mathbf{u} = 0$, which, combined with (1) and (2), shows that the pressure in the sea ice is determined by $[\beta^2 \partial^2/\partial x^2 - \gamma \partial/\partial z + \partial^2/\partial z^2] p = 0$ and is equal to

$$p = -\rho\alpha U^2 \zeta e^{qz}, \tag{7}$$

where $q = \gamma/2 + \frac{1}{2}\sqrt{\gamma^2 + 4\alpha^2\beta^2}$. If we take the temperature in the sea ice to be $T = Gz + \hat{\theta}(z)e^{i\alpha x + \sigma t}$, a perturbation from a linear temperature gradient, the quasi-stationary approximation of the heat equation in the sea ice (3) gives

$$\kappa(\frac{d^2}{dz^2} - \alpha^2)\hat{\theta} = \frac{G\Pi_\nu(0)}{\nu}\alpha q U^2 \hat{\zeta} e^{(q+\gamma)z}, \tag{8}$$

where $\kappa \equiv k/(\rho c)$ is the thermal diffusivity and $\nu \equiv \mu/\rho$ is the kinematic viscosity of the ocean (and interstitial brine). The quasi-stationary approximation essentially implies that the sea ice grows/decays sufficiently slowly that the temperature (and hence solid fraction) fields evolve to the equilibrium, steady state profiles for the boundary conditions. A numerical study [*Feltham and Worster*, 1999] shows the quasi-stationary approximation to be a useful approximation which yields accurate stability curves. The quasi-stationary heat equation has solution

$$\hat{\theta} = \frac{G\Pi_\nu(0)U^2}{\kappa\nu} \frac{\alpha q}{(q+\gamma)^2 - \alpha^2} \zeta(e^{(q+\gamma)z} - e^{\alpha z}) - G\hat{\zeta}e^{\alpha z}. \tag{9}$$

Note that at the interface T is fixed at the freezing point which is normalized here to zero and as the denominator in (9) tends to zero ($\beta \to 1$, $\gamma \to 0$), we obtain

$$\lim_{\beta \to 1, \gamma \to 0} \hat{\theta} = \frac{G\Pi_\nu(0)U^2}{2\kappa\nu}\hat{\zeta}\alpha z e^{\alpha\beta z} - G\hat{\zeta}e^{\alpha z}. \tag{10}$$

Finally, the Stefan condition (4) gives

$$\sigma = \frac{k}{\rho\mathcal{L}\phi}\alpha G[-1 + \frac{\Pi_\nu(0)}{\kappa\nu}\frac{qU^2}{q+\gamma+\alpha}], \tag{11}$$

where we have ignored the perturbed heat flux from the ocean since a fuller analysis [*Feltham and Worster*, 1999] shows it to have only a minor effect on the growth of perturbations although it causes the corrugations to translate in the direction of the mean, oceanic flow. The simple analysis presented here
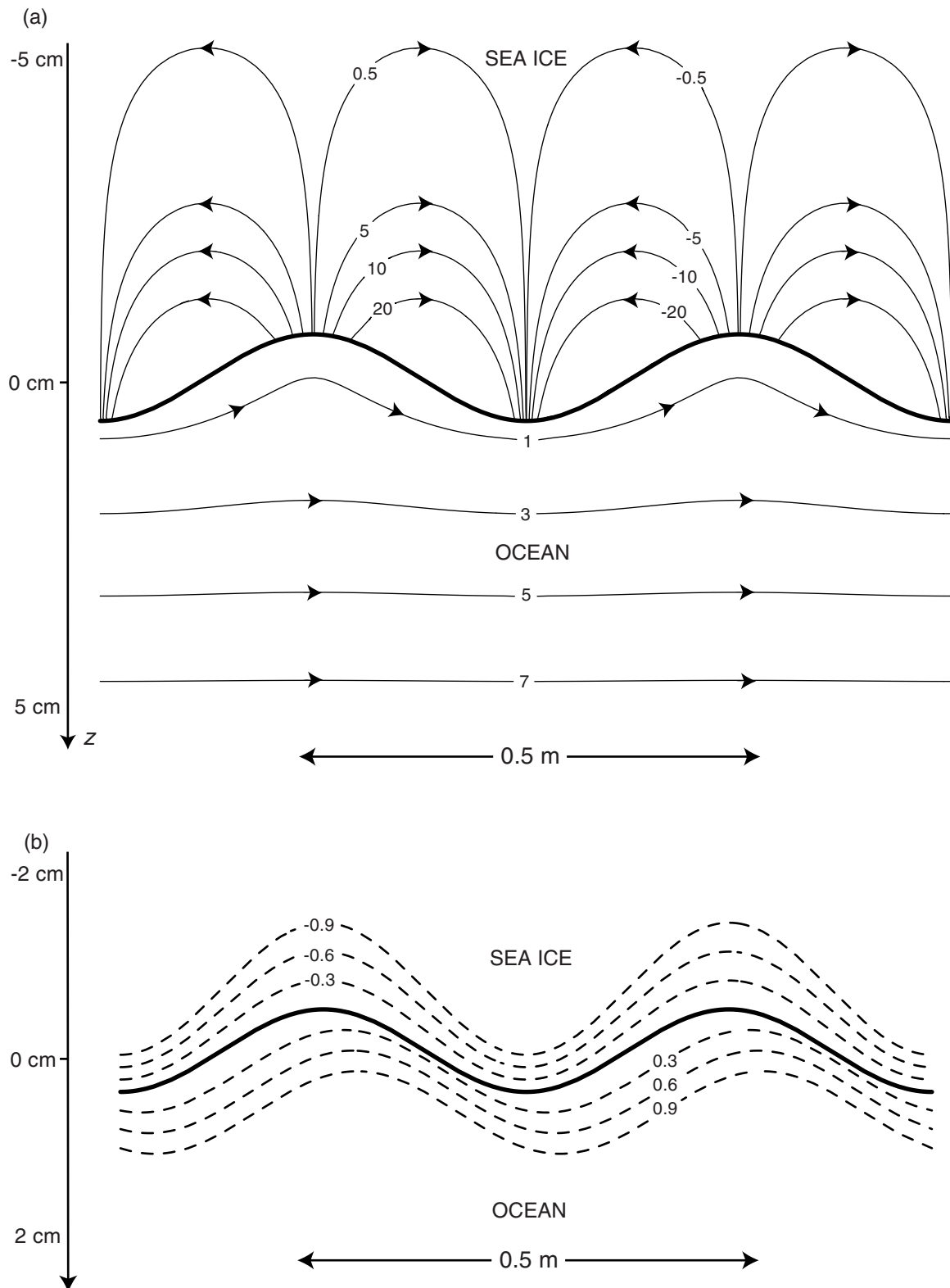
Figure 3. (a) Schematic diagram showing the secondary flow in the sea ice and ocean and representative magnitudes. The contour levels of the stream function in the sea ice are in units of $10^{-10}m^2 \ s^{-1}$, and the contour levels of the stream function in the ocean are in units of $10^{-4}m^2 \ s^{-1}$. (b) Schematic diagram indicating the effect of the secondary flow on the isotherms in the sea ice and ocean and representative magnitudes. The isotherms are labeled with the temperature difference in Kelvins from the interfacial temperature, taken to be the freezing point of seawater. See text for discussion.
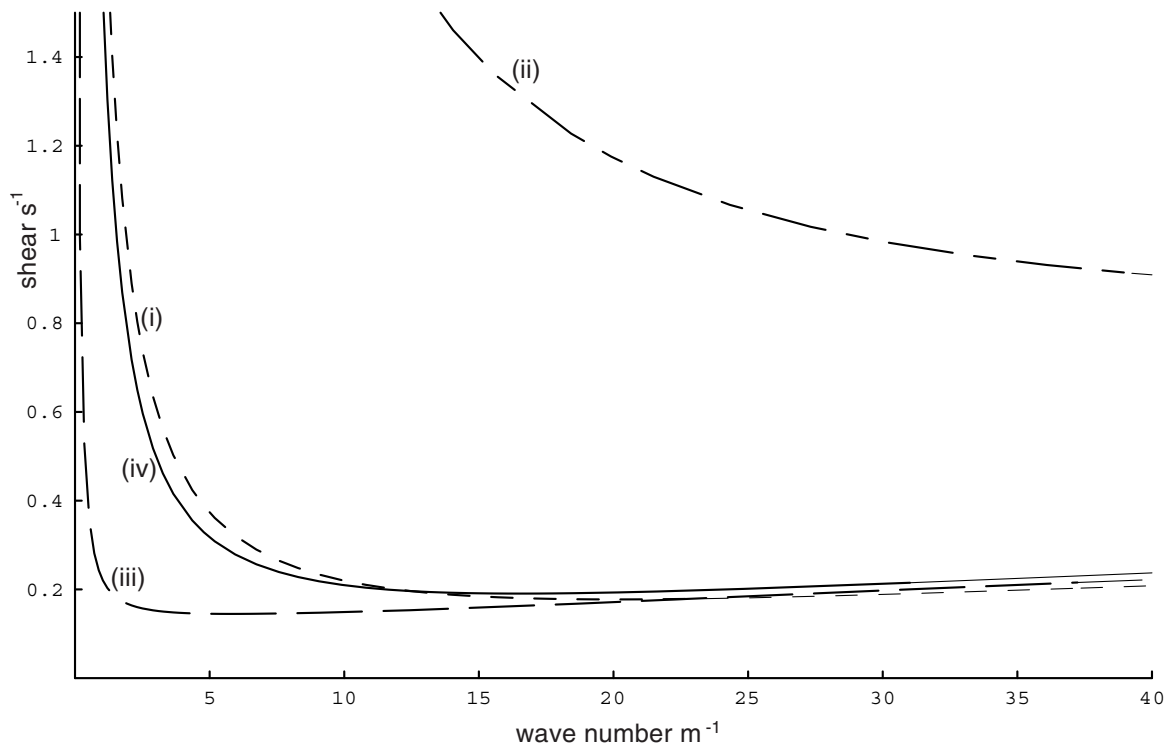
Figure 4. Plots of critical oceanic shear versus wave number for isotropic, homogeneous permeability ($\beta = 1$, $\gamma = 0$ cm^{-1}) (short-dashed line, labeled i); anisotropic, homogeneous permeability ($\beta = 0.1$, $\gamma = 0$ cm^{-1}) (long-and-short-dashed line, labeled ii); isotropic, heterogeneous permeability ($\beta = 1$, $\gamma = 1$ cm^{-1}) (long-dashed line, labeled iii); and anisotropic, heterogeneous permeability ($\beta = 0.1$, $\gamma = 1$ cm^{-1}) (solid line, labeled iv).

shows that the incipient corrugation grows, and hence there is an instability, if the dimensionless group

$$\frac{\prod_v(0)U^2}{\kappa\nu} > \frac{q + \gamma + \alpha}{q}; \qquad (12)$$

that is, if the external flow is sufficiently rapid. In the special case of permeability independent of depth ($\gamma \to 0$), we obtain the even simpler criterion

$$\frac{\prod_{\mathbf{eff}}U^2}{\kappa\nu} > 1 + \beta, \qquad (13)$$

where the effective permeability $\prod_{\mathrm{eff}} \equiv (\prod_v\prod_h)^{1/2}$ is defined as the geometric mean of the permeability parallel and perpendicular to the ice platelets.

[7] The effect of the flow on the isotherms in the ocean and sea ice is shown schematically in Figure 3b. While in the sea ice it is brine flow which modifies the isotherms, in the ocean this brine flow is negligible in comparison with the secondary flow caused by the interaction of a uniform flow with a corrugated interface. Thus the effect of flow on the isotherms in the ocean is essentially that due to flow past an impermeable interface, such as solid ice. In the ocean the isotherms are compressed at the upstream face of each crest and rarefied at the downstream face. This causes the upstream face to melt and the downstream face to freeze, which gives a translation of the interface shape in the direction of the basic flow. Thus the effect of the flow in the ocean is to translate corrugations but not to cause them to grow or decay. There is experimental evidence of such downstream migration given by *Gilpin et al.* [1980], who investigated the effects of water flowing past corrugations in a layer of solid ice.

The isotherms in the sea ice, however, are compressed near the crests by the induced brine flow, which enhances conduction of heat away from the sea ice–ocean interface and promotes its advance. Conversely, the isotherms at the troughs are rarefied, and the advance of the interface is retarded. This is the mechanism by which flow over the sea ice–ocean interface can cause the interface to become unstable. Note that, in the absence of advection by brine, the effect of thermal diffusion is to stabilize the sea ice–ocean interface so that the perturbations decay.

[8] We have considered a modification of the analysis of *Feltham and Worster* [1999]; they considered a finite-depth mushy layer growing at constant rate into its melt with the flow in the melt given by the full Navier-Stokes equations. They found that long-wavelength corrugations are stable because of the weakness of Bernoulli suction, that the short wavelength corrugations are stable when the external flow is a viscous shear rather than an inviscid uniform flow, and that the most unstable wavelengths are about 3–4 times the depth of the mushy layer. A limitation to this work, however, was that they considered the permeability of the mushy layer to be isotropic and homogeneous (essentially, they considered $\beta \to 1$, $\gamma \to 0$ cm^{-1}). Here we present new calculations in order to represent the anisotropy ($\beta < 1$) and spatial dependence ($\gamma > 0$ cm^{-1}) of the permeability in sea ice. The details of the calculations are similar to those described by *Feltham and Worster* [1999], to which the interested reader is referred. Essentially, the perturbed Navier-Stokes equations are solved in the ocean semianalytically to obtain the perturbed pressure at the sea ice–ocean interface. The perturbed pressure is used to calculate the brine flow and advection of heat and salt (which are linked by the liquidus curve) in the sea ice using Darcy's law and local conservation of heat and mass. Finally, the Stefan condition is used to determine the critical oceanic shear for instability to occur. Although all of these calculations are mutually dependent in principle, the vastly differ-
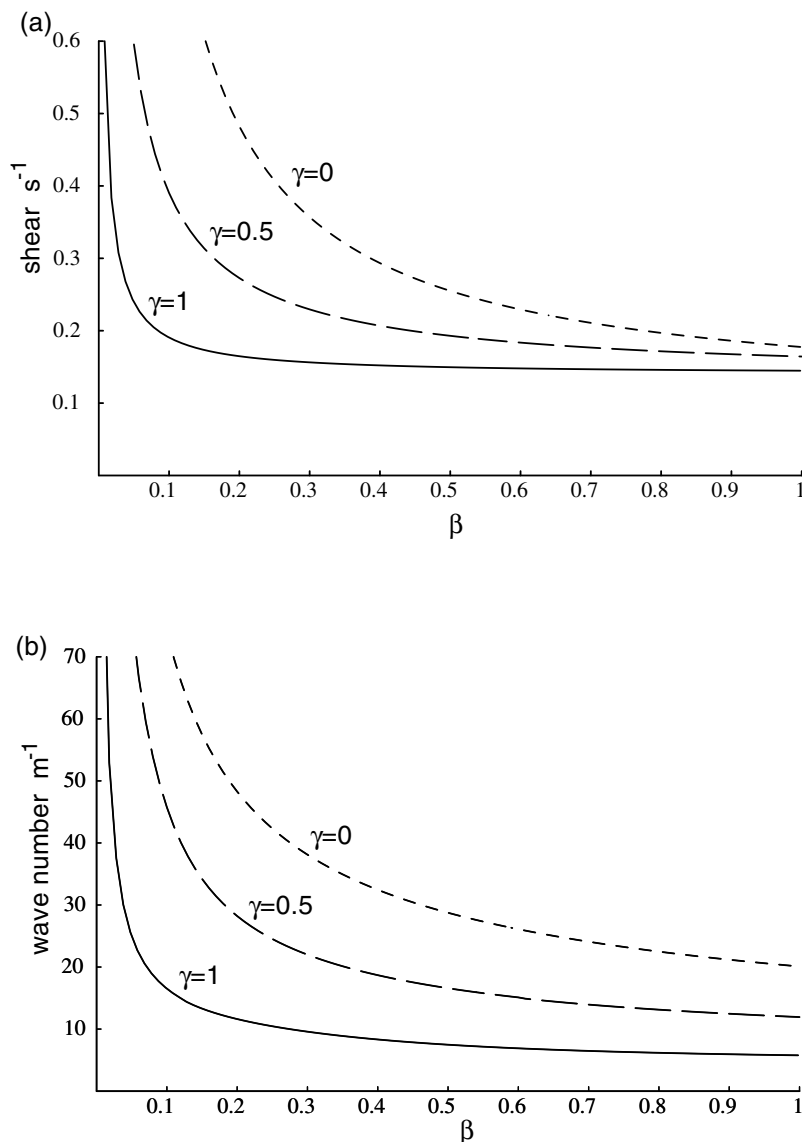
Figure 5. (a) Plot of minimum critical oceanic shear required to cause instability versus β for $\gamma = 0$, 0.5 and 1 cm^{-1} (short-dashed, long-dashed, and solid lines, respectively). (b) Plot of critical wave number (the wave number that corresponds to the minimum oceanic shear required for instability) versus β for $\gamma = 0$, 0.5 and 1 cm^{-1} (short-dashed, long-dashed, and solid lines, respectively).

ent scales of variation of flow in the ocean and sea ice allow them to be performed sequentially. In Figure 4 we show plots of critical oceanic shear versus wave number for (1) isotropic, homogeneous permeability ($\beta = 1$, $\gamma = 0$ cm^{-1}) (short-dashed line, labeled i) which reproduces the results of *Feltham and Worster* [1999] (though here the neutral curve is expressed in terms of dimensional shear and we use a higher permeability); (2) anisotropic, homogeneous permeability ($\beta = 0.1$, $\gamma = 0$ cm^{-1}) (long-and-short-dashed line, labeled ii); (3) isotropic, heterogeneous permeability ($\beta = 1$, $\gamma = 1$ cm^{-1}) (long-dashed line, labeled iii); and (4) anisotropic, heterogeneous permeability ($\beta = 0.1$, $\gamma = 1$ cm^{-1}) (solid line, labeled iv), which we take to be representative of newly forming sea ice. For values of shear above the curve appropriate to the permeability structure, the instability will be triggered. The parameters used to calculate these curves are $\mu = 1.1 \times 10^{-3}$ kg m^{-1}s^{-1}, $\rho = 1.027 \times 10^3$ kg m^{-3} (giving $\nu = 1.07 \times 10^{-6}$m^2 s^{-1}), $\kappa = 1.33 \times 10^{-7}$m^2 s^{-1}, a sea ice growth rate of 10^{-6}m s^{-1}, and an ice depth of 7 cm (the arguments and sources for these parameter values are given by *Feltham* [1997]). There is little data available on the value of the vertical component of permeability at the sea ice–ocean interface $\Pi_v(0)$, and we set $\Pi_v(0) = 10^{-8}$ m^2 which was estimated in the following manner. Values extracted from field data for ice newly formed in leads [*Wettlaufer et al.*, 2000] suggest a permeability of $\Pi(\bar{\phi}) \approx 10^{-10}$m^2 where $\bar{\phi}$ is the vertically averaged solid fraction in the sea ice layer. Assuming that $\Pi(\phi) \approx (1/h) \int_0^h \Pi_{\mathrm{eff}}(z)dz$ allows one to calculate that $\Pi_v(0) \approx (\gamma h/\beta) \Pi(\phi) \approx 10^{-8}$m^2, where we have taken $\beta \approx 0.1$ and $\gamma \approx 1$ cm^{-1}and the ice depth $h = 7$ cm. These values are consistent with other observations [*Freitag*, 1999; *Saiki et al.*, 1986]. For sea ice we have taken $\gamma = 1$ cm^{-1} from *Ono and Kasai* [1980], where we set a typical temperature gradient in newly forming sea ice to be ≈ 1 K cm^{-1}; the value chosen for β (corresponding to $_h = 0.01 _v$) is an estimate since little data is available. The dependence of the instability upon β is shown in Figure 5a (where $_v(0) = 10^{-8}$ m^2 is treated as constant), which shows the variation of the minimum critical oceanic shear required to cause instability versus β for $\gamma = 0$, 0.5 and 1 cm^{-1} (short-dashed, long-dashed, and solid lines, respectively). In Figure 5b we
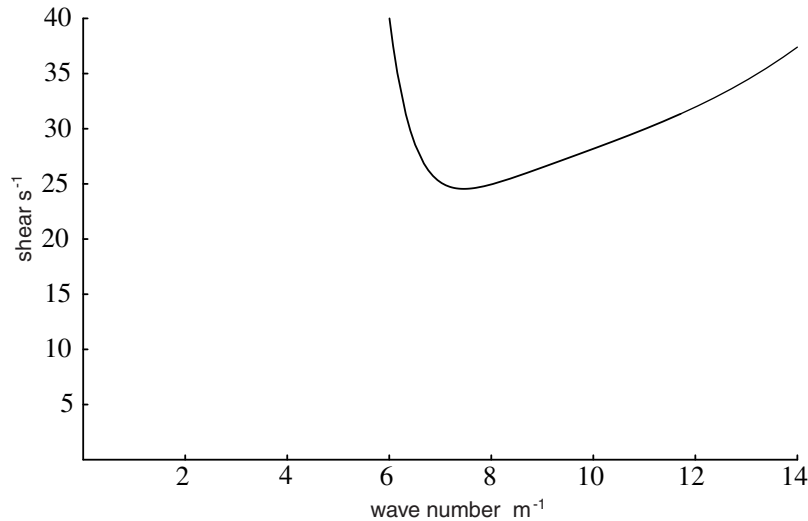
Figure 6. Plot of critical oceanic shear versus wave number for *Gilpin et al.'s* [1980] mechanism. The shear rate required for instability is approximately 125 times that required for the mechanism presented in this paper.

show the critical wave number, the wave number that corresponds to the minimum oceanic shear required for instability, versus β for $\gamma = 0$, 0.5 and 1 cm^{-1} (short-dashed, long-dashed, and solid lines, respectively). From Figure 4 we see from comparison of curve iii, isotropic and heterogeneous permeability, with curve i, isotropic and homogeneous permeability, that strong attenuation of permeability in the sea ice away from the ice-ocean interface strengthens the instability (decreases the minimum shear required for instability) and decreases the critical wave number at which instability is most likely to occur. Since $\gamma > 0$ cm^{-1} corresponds to the brine flow in the sea ice being focused into the region adjacent to the ice-ocean interface, we expect the brine speed to be increased, advecting more heat and thus strengthening the instability. Comparison of curve ii with curve i in Figures 4, 5a, and 5b, shows that as β is reduced below unity, the instability is weakened and the critical wave number is increased. This effect is expected since the horizontal transport and horizontal length scale of brine flow from troughs to crests (see Figure 3b) is decreased, reducing advection of heat and the effective wavelength of the circulation. In curve iv of Figure 4, anisotropy and heterogeneity are combined, and we see that to a great extent the opposing effects cancel, leaving a stability curve quite similar to curve i, the homogeneous and isotropic case investigated by *Feltham and Worster* [1999]. From Figure 4, curve iv, and Figure 5a, we see that for the above parameters we would expect the instability to be triggered in newly forming sea ice for an oceanic shear rate at the ice interface of about 0.2 s^{-1}, which corresponds to an ocean flow rate external to a viscous boundary layer with depth 10 cm of about 2 $cm\ s^{-1}$. This is well within the range typically encountered during, for example, the Arctic Ice Dynamics Joint Experiment (AIDJEX) [*McPhee*, 1986], the Coordinated Eastern Arctic Experiment (CEAREX) [*Omstedt and Wettlaufer*, 1992] and the Arctic Leads Experiment (LEADEX) [*McPhee and Stanton*, 1996], and thus, even accounting for errors of a factor of 10, we expect the instability to be triggered in many situations. For the above parameters, the critical wave number is about 17 m^{-1}, corresponding to an expected wavelength of corrugations of 40 cm or about 5 times the sea ice depth.

3. Discussion

[9] An understanding of the interaction between the oceanic boundary layer and the morphological evolution of the underside

of sea ice is basic to the heat and mass balance in ice-covered seas. The hydraulic roughness of sea ice exerts a controlling influence on the boundary layer dynamics and hence the heat and mass fluxes at the ice-ocean interface [e.g., *McPhee*, 1992; *Omstedt and Wettlaufer*, 1992]. Additionally, latent heat released by the growth of corrugations on the underside of sea ice results, because the ice-ocean interface is treated as flat, in significant horizontal variations in computed oceanic heat flux as the ice cover thickens [*Wettlaufer*, 1991]. Therefore uncovering potential mechanisms that underlie an increase or decrease of the roughness of sea ice is of geophysical relevance, and this is particularly important in the case of first year ice, which dominates the wintertime heat balance.

[10] We have described a new mechanism whereby a sufficiently rapid oceanic flow can give rise to a corrugated sea ice–ocean interface. The mechanism relies on brine flows developing within the sea ice in response to Bernoulli suction caused by boundary layer flow adjacent to the interface. It has been suggested [*Wettlaufer*, 1991] that the formation of corrugations on the underside of perennial sea ice could occur because of the instability mechanism described by *Gilpin et al.* [1980]. Gilpin et al. presented an instability of a pure-ice–melt interface due to a turbulent flow in the melt. If the turbulent heat flux into the ice-melt interface is out of phase with the incipient corrugations by greater than $\pi/2$ and less than π, then the heat flux is enhanced near troughs and retarded near crests. This causes the corrugations to grow and move downstream. In Figure 6 we present the curve of critical shear versus wave number for Gilpin et al.'s mechanism for ice of 7 cm depth in a stationary state (we use Gilpin et al.'s $G = 1$ curve; they define G to be the ratio of the unperturbed heat into the ice-water interface from the water to the heat out of the interface through the ice). This is the appropriate curve of critical shear with which to compare the stability curves obtained in this paper. The comparison of Figure 6 and curve iv of Figure 4 clearly demonstrates that the mechanism described in this paper is likely to be more effective than that of Gilpin et al. for newly forming sea ice since it requires an oceanic shear smaller by a factor of approximately 125. Since the most likely corrugation wavelengths differ for the two mechanisms, this may be a way to distinguish which, if either, is responsible for any observed corrugations.

[11] We have described the mechanism presented in this paper using a linear stability analysis; this can only indicate if an incipient corrugation will grow or decay. However, we may

speculate that the growth of corrugations will initially continue to be dominated by brine flow in the sea ice. One argument against this, however, is that as heat and salt is advected by flow in the sea ice, the solid fraction increases, which decreases the permeability and thus weakens the driving force for growth of corrugations. A crude estimate of the timescale for this to occur can be obtained by balancing the advection and phase change terms in the heat conservation equation (3), $\rho c \mathbf{u} \cdot \nabla T \sim \rho \mathcal{L} \partial \phi / \partial t$. Using Darcy's law (1) and the Bernoulli expression for pressure (6), it is seen that $\mathbf{u} \cdot \nabla T \sim G \, \Pi \alpha U^2 \delta^2 / (\nu \lambda^2)$, where δ and λ are the amplitude and wavelength of the corrugations, respectively. Then, we see that $\Delta t \sim \Delta \phi (\mathcal{L} \nu \lambda^3) / (2 \pi c G \Pi U^2 \delta^2)$. Inserting $\Pi = 10^{-8} \text{ m}^2$, $c = 4.2 \times 10^3 \text{ J kg}^{-1} \text{ K}^{-1}$, $\mathcal{L} = 3.5 \times 10^5 \text{ J kg}^{-1}$ [*Feltham*, 1997], $U = 0.02 \text{ m s}^{-1}$, $\Delta \phi = 0.5$, $\delta = 10^{-2}$ m, $\lambda = 0.4$ m and $G = 100 \text{ K m}^{-1}$, we obtain $\Delta t \approx 10^7$ s (100 days). Although we would expect the reduction of permeability to play an important role before this, it does suggest that provided the growth rate of the sea ice is sufficiently rapid, the increase in solid fraction will not affect the ice that is newly forming at the ocean boundary. Assuming that the corrugations form by the mechanism presented in this paper, the growth rate for incipient corrugations is given by $[c\kappa / (\mathcal{L}\phi) \partial \hat{\theta} / \partial z (z = 0)]$. Although this expression is strictly only valid for infinitesimal corrugations, we use it to estimate the growth rate of corrugations which have a small amplitude relative to the depth of the ice layer. Treating the ocean flow as a viscous shear rather than a uniform flow results in a growth rate approximately an order of magnitude smaller than that predicted by (11) for the critical wave number [*Feltham and Worster*, 1999]. Inserting the parameters used to generate curve iv in Figure 4, and using the parameters above, we obtain $\zeta^{-1} d\zeta / dt \approx 10^{-5} \text{ s}^{-1}$ which is relatively insensitive to β in the range $[10^{-3}, 10^3]$. This simple approach suggests that a 1-cm corrugation will grow to about 2.5 cm in 12 hours. This growth rate is similar to (and slightly larger than) the growth rate estimated by *Wettlaufer* [1991] for *Gilpin et al.*'s [1980] mechanism. Such corrugations will affect the turbulent transfers of heat, mass, and momentum (the momentum transfer from the ocean to the ice layer through oceanic surface drag is the main contribution to total oceanic drag between distinct features such as the keels of pressure ridges). The effect of corrugations on these transfers is parameterized through the surface roughness length in the well-known logarithmic law for the surface layer of the oceanic boundary layer; for example, *Mellor et al.* [1986] set the roughness length for momentum to be $z_0 \approx \delta/30$, where δ is the size of a typical perturbation (the equivalent lengths for heat and salinity were slightly smaller). In addition to the effect on the surface roughness length the growth of corrugations results (for the above growth rate) in variations in the latent heat flux of $\approx 20 \text{ W m}^{-2}$, and hence variations in the calculated oceanic heat flux, on horizontal spatial scales several times larger than the region of appreciable permeability, for example, 40 cm. The eventual fate of such corrugations is difficult to predict. Once a steady oceanic shear is removed, the corrugations will tend to flatten out due to diffusion of heat within the sea ice at a rate approximately given by (11) with $U = 0$. For example, a 2.5-cm corrugation will reduce to 2 cm after 12 hours of quiescence. However, if a current changes sign but maintains its orientation, the corrugations will continue to grow but will reverse their direction of translation. The presence and size of corrugations thus clearly depends upon the recent history of flow beneath a sea ice layer. We may speculate, for example, that a period of persistent flow in one direction directly followed by a persistent flow in an orthogonal direction might lead to the formation of a grid of hummocks and valleys. The instability mechanism described in this paper may also trigger buoyancy-driven circulation within sea ice by bringing dense brine to the same depth as adjacent, less dense ocean water. Experiments [*Wettlaufer et al.*, 1997a, 1997b] and detailed numerical simulations [*Schulze and Worster*, 1999] show that such buoyancy-driven circulations can ultimately create brine channels.

[12] The conditions required for the instability to be triggered are such that we might expect corrugations to commonly form during the formation of sea ice where there is a moderate to strong shear flow in the ocean. In particular, the corrugations are likely to form during storms in the central Arctic Ocean, in ice-covered tidally driven fjords, in coastal polynyas where the magnitude of the wind drift is large, and in leads where haline convection is taking place [*Smith and Morison*, 1993].

[13] Evidence might be sought under leads during storms, in Van Mijen fjord in Svalbard, the wind-driven polynya off the north Greenland coast or between the Henrik Kroyer islands and the Ob Bank. Further laboratory experiments and field observations will allow detailed tests of our predictions.

References

Aagaard, K., and E. Carmack, The arctic ocean and climate: A perspective, in *The Polar Regions and Their Role in Shaping the Global Environment, Geophys. Monogr. Ser.*, vol. 85, edited by O. M. Johannessen, et al., pp. 5–20, AGU, Washington, D. C., 1994.

Batchelor, G. K., *An Introduction to Fluid Dynamics*, Cambridge Univ. Press, New York, 1967.

Bear, J., *Dynamics of Fluids in Porous Media*, Elsevier Sci., New York, 1972.

Ebert, E. E., and J. Curry, An intermediate one-dimensional thermodynamic sea ice model for investigating ice-atmosphere interactions, *J. Geophys. Res.*, 98, 10,085–10,109, 1993.

Feltham, D. L., Fluid dynamics and thermodynamics of sea ice, Ph.D. thesis, Univ. of Cambridge, Cambridge, United Kingdom, 1997.

Feltham, D. L., and M. G. Worster, Flow-induced morphological instability of a mushy layer, *J. Fluid Mech.*, 391, 337–357, 1999.

Freitag, J., The hydraulic properties of Arctic sea ice – Implications for the small-scale particle transport (in German), *Ber. Polarforsch. 325,* 150 pp., Alfred-Wegener-Inst. fur Polar- und Meeresforsch., Bremerhaven, Germany, 1999.

Gilpin, R. R., T. Hirata, and K. G. Cheng, Wave formation and heat transfer at an ice-water interface in the presence of turbulent flow, *J. Fluid Mech.*, 99, 619–640, 1980.

Maykut, G. A., and N. Untersteiner, Some results from a time-dependent, thermodynamic model of sea ice, *J. Geophys. Res.*, 76, 1550–1575, 1971.

McPhee, M. G., The oceanic boundary layer, in *The Geophysics of Sea Ice*, chap. 4, *NATO ASI Ser. B*, 146, 1986.

McPhee, M. G., Turbulent heat flux in the upper ocean under sea ice, *J. Geophys. Res.*, 97, 5365–5379, 1992.

McPhee, M. G., and T. P. Stanton, Turbulence in the statically unstable oceanic boundary layer under Arctic leads, *J. Geophys. Res.*, 101, 6409–6428, 1996.

McPhee, M. G., T. P. Stanton, J. H. Morison, and D. G. Martinson, Freshening of the upper ocean in the arctic: Is perennial sea ice disappearing?, *Geophys. Res. Lett.*, 25, 1729–1732, 1998.

Mellor, G. L., M. G. McPhee, and M. Steele, Ice-seawater turbulent boundary layer interaction with melting and freezing, *J. Phys. Oceanogr.*, 16, 1829–1846, 1986.

Morison, J. H., M. Steele, and R. Andersen, Hydrography of the upper ocean in the arctic measured from the nuclear submarine U.S.S. Pargo, *Deep Sea Res. Part I*, 45, 15–38, 1998.

Ono, N., and T. Kasai, Surface layer salinity of young sea ice, *Ann. Glaciol.*, 6, 298–299, 1980.

Omstedt, A., and J. S. Wettlaufer, Ice growth and oceanic heat flux: Models and measurements, *J. Geophys. Res.*, 97, 9383–9390, 1992.

Phillips, O., *Flow and Reactions in Permeable Rocks*, Cambridge Univ. Press, New York, 1991.

Rothrock, D. A., Y. Yu, and G. A. Maykut, Thinning of the arctic sea-ice cover, *Geophys. Res. Lett.*, 26, 3469–3472, 1999.

Saiki, H., T. Takeuchi, M. Sakai, and E. Suenaga, Experimental study on permeability coefficient of sea ice, in *Proceedings of International Conference on Ice Technology*, pp. 237–246, Springer-Verlag, New York, 1986.

Schulze, T. P., and M. G. Worster, Weak convection, liquid inclusions and

the formation of chimneys in mushy layers, *J. Fluid Mech.*, *388*, 197–215, 1999.

Semtner, A. J., A model for the thermodynamic growth of sea ice in numerical investigations of climate, *J. Phys. Oceanogr.*, *6*, 379–389, 1976.

Smith, D. S., and J. H. Morison, A numerical study of haline convection beneath leads in sea ice, *J. Geophys. Res.*, *98*, 10,069–10,083, 1993.

Untersteiner, N., Natural desalination and equilibrium salinity profile of sea ice, *J. Geophys. Res.*, *73*,1251–1257, 1968.

Weeks, W. F., Growth conditions and the structure and properties of sea ice, in *Physics of Ice-Covered Seas*, edited by M. Leppäranta, pp. 24–104, Univ. of Helsinki Press, Helsinki, 1998.

Wettlaufer, J. S., Heat flux at the ice-ocean interface, *J. Geophys. Res.*, *96*, 7215–7236, 1991.

Wettlaufer, J. S., M. G. Worster, and H. E. Huppert, The phase evolution of young sea ice, *Geophys. Res. Lett.*, *24*, 1251–1254, 1997a.

Wettlaufer, J. S., M. G. Worster, and H. E. Huppert, Natural convection during solidification of an alloy from above with application to the evolution of sea ice, *J. Fluid. Mech.*, *344*, 291–316, 1997b.

Wettlaufer, J. S., M. G. Worster, and H. E. Huppert, Solidification of leads: Theory, experiment, and field observations, *J. Geophys. Res.*, *105*, 1123–1134, 2000.

Zhang, J., W. D. Hibler, III, M. Steele, and D. A. Rothrock, Arctic ice-ocean modeling with and without climate restoring, *J. Phys. Oceanogr.*, *28*, 191–217, 1998.

―――――――――

D. L. Feltham, Centre for Polar Observation and Modelling, Department of Space and Climate Physics, University College London, Gower Street, London WC1E 6BT, UK. (Daniel.Feltham@cpom.ucl.ac.uk)

J. S. Wettlaufer, Departments of Geology and Geophysics and Physics, Yale University, New Haven, CT 06520, USA. (john.wettlaufer@yale.edu)

M. G. Worster, Institute of Theoretical Geophysics, Department of Applied Mathematics and Theoretical Physics, University of Cambridge, Silver Street, Cambridge CB3 9EW, UK. (grae@esc.cam.ac.uk)